

Full Length Research Paper

Application of Landsat imagery for landuse/landcover analyses in the Afikpo sub-basin of Nigeria

*Chukwu G. U., Ijeh B. I. and Olunwa K. C.

Department of Physics, Michael Okpara University of Agriculture, Umudike, Abia State, Nigeria.

Accepted February 26, 2013

Lately, several remote sensing data types are now available for geological and environmental studies. The variety has increased as many nations including some African countries invest in satellite remote sensing. However, each data type has its own peculiar features that may limit or enhance its relevance to capture data for specific range of information. This study used geo-information techniques based on the Landsat imagery to enhance the utilization of images with coarser resolutions in land use analysis in Afikpo sub-basin which lies within the Benue Trough of Nigeria. The objective of the study is to evaluate the lineament analysis, structural interpretation and variations in land use characterization with the satellite data source in Afikpo sub-basin which is located within latitude $6^{\circ} 00'$ and $5^{\circ} 30'N$ and longitude $7^{\circ} 30'$ and $8^{\circ} 00'E$. The remotely sensed data sets used are the Landsat imagery of NigeriaSat-2 2012 satellite. Several GIS software which includes the ILWIS 3.2, SURFER 10, ERDAS, and DIGIER 5.0 were used to analyze the data sets. It was found that the Mamu Formation in the sub-basin could be a potential site for mineral exploration with high lands up to 277 meters above mean sea level and also the Asu River Group Formation could be a possible hydrocarbon reservoir. Ajali Formation was also discovered to be prone to severe tectonic activities.

Keywords: lineament analysis, structural interpretation, Landsat imagery, Afikpo sub-basin, Benue trough

INTRODUCTION

Geophysical techniques and remote sensing have been used for geologic interpretations with remarkable success. Remote sensing techniques are used because of their cost effectiveness, their ability to access areas that are difficult to access and because the data can be collected frequently and rapidly on a large scale. These data sets allow earth-based phenomena such as land use and land cover characteristics to be rapidly mapped, if needed repetitively and at relatively low costs. With increasing capacity to rapidly generate maps of large areas, planners in the rural and urban areas are getting more empowered to address issues associated with land use analysis such land misuse and various forms of incursion into properties and trespassing. Remote sensing refers to the activities of recording, observing, and perceiving objects or events in far-away (remote)

places. In a more restricted sense, remote sensing refers to the science and technology of acquiring information about the earth's surface (i.e. land and ocean) and atmosphere using sensors onboard airborne (e.g. aircraft or balloons) or space borne (e.g. satellites and space shuttles) platforms. In remote sensing, the sensors are not in direct contact with the objects as the information carrier in remote sensing. The output of a remote sensing system is usually an image representing the scene being observed. A further step of image analysis and interpretation is required to extract useful information from the image. Depending on the scope, remote sensing may be broken down into:

- (1) Satellite remote sensing (when satellite platforms are used),
- (2) Photography and photogrammetry (when photographs are used to capture visible light),
- (3) Thermal remote sensing (when the thermal infrared portion of the spectrum is used),
- (4) Radar remote sensing (when microwave wavelengths are used), and
- (5) LIDAR remote sensing (when laser pulses are trans-

*Corresponding Author E-mail: chukwug@yahoo.com

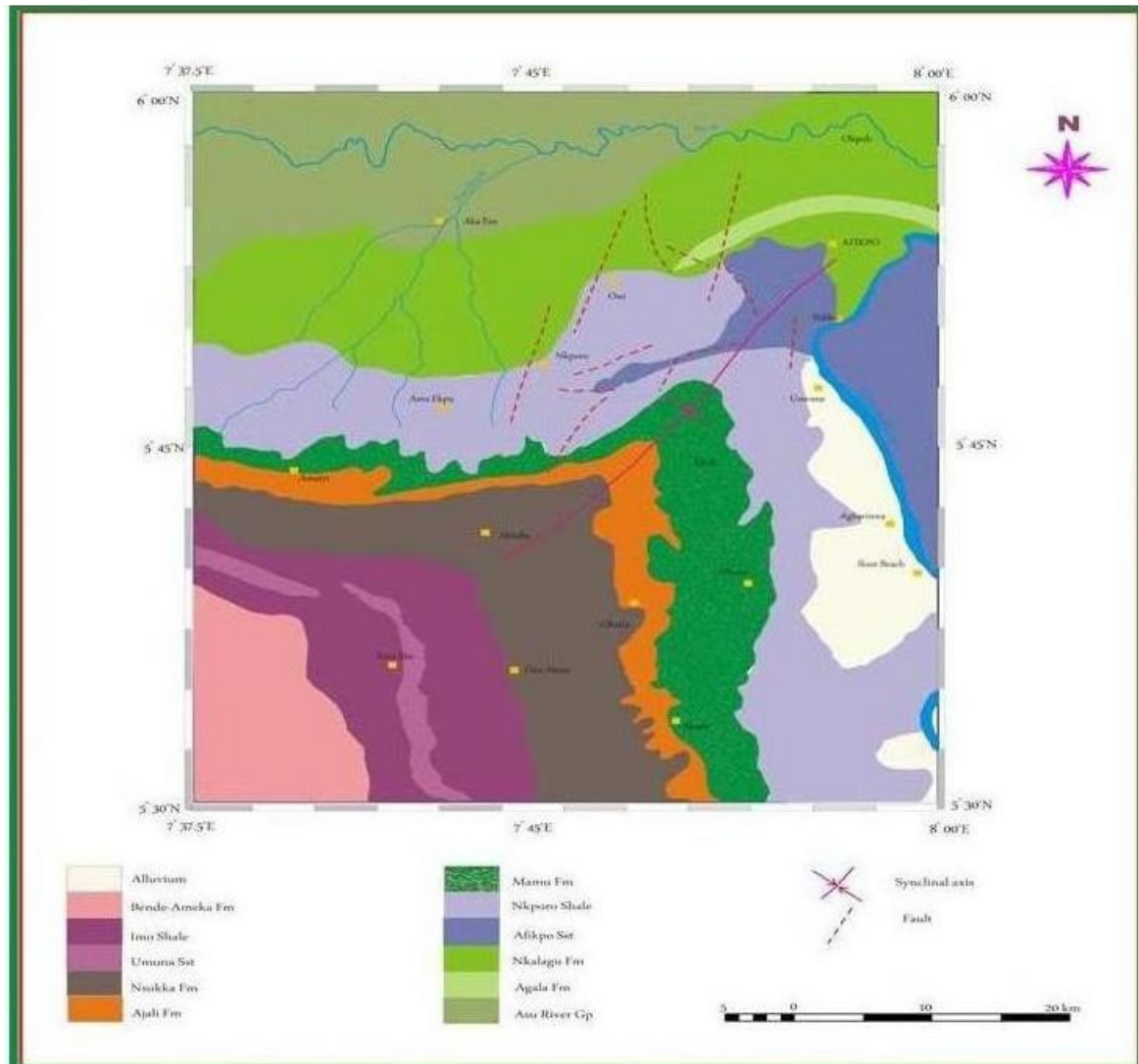


Figure 1. Geology map of the study area

mitted toward the ground and the distance between the sensor and the ground is measured based on the return time of each pulse) (Ojo and Adesina, 2007).

Some of the most commonly used remote sensing data sets for mapping land use and land cover are those from Landsat, SPOT (Système Probatoire d'Observation de la Terre), IRS (Indian Remote Sensing), ASTER (Advanced Space-borne Thermal Emission and Reflection Radiometer), MODIS (Moderate Resolution Imaging Spectrometer), JERS-1 (Japanese Earth Resources Satellite), NigeriaSat-1 and recently, NigeriaSat-2 satellites. The Landsat data have greater spectral resolution (Gastellu-Etchegorry, 1990) and a longer time series, while SPOT provides better spatial resolution but with shorter historical records. Newer satellite imaging systems are commonly equipped with enhanced instruments to generate additional data that permit more accurate mapping and analysis. Land

use/land cover analyses usually proceed from classification of the area of study. The classified units can be further analyzed in terms of their characteristics particularly size. Factors that may influence classification accuracy include a sensor's spatial, radiometry and spectral resolutions. Spatial resolution describes the size each pixel represents in the real world (Cushnie, 1987). For example, a satellite with 30 meter resolution produces pixels that measures a 30x30 meter area on the ground. Radiometric resolution, on the other hand, is the smallest difference in brightness that a sensor can detect. A sensor with high radiometric resolution would therefore have very low "noise". The "noise" is described as any unwanted or contaminating signal competing with the desired signal.

Spectral resolution is the number of different wavelengths that a sensor can detect. A sensor that produces a panchromatic image alone has a very low

spectral resolution, while one that can distinguish many shades of each color has a high spectral resolution (Jensen, 2007).

Geology of the study area

Afikpo sub-basin is located in the southeastern part of the sedimentary basin lower Benue Trough. The Afikpo basin is situated in the southeastern Nigeria and it covers about 60, 000 square km. The Afikpo Basin represents an elongate NE-SW depocenter.

The sedimentary fill in the Afikpo basin is divided into three tectonic-stratigraphic mega sequences the Asu River Group, Eze-Aku Group and proto-Niger Delta succession. The detailed stratigraphic succession is presented in Figure 1.

The Asu River Group, consisting of shale, sandstone, and limestone, is the older lithostratigraphic unit in the area and was deposited during Albian transgressive phase. It is also the oldest dated sedimentary rock unit in southern Benue Trough (Whiteman, 1982). Simpson (1955), and Reymont and Barber (1956) were of the view that the Asu River Group was deposited in a moderately deep water environment during the Albian, with abundant ammonites, floras, radiolarian, and pollens.

According to Reymont (1965), the Albian sediments were moderately folded in many places with the fold axes trending NE-SW. The Nkporo Formation in the Afikpo syncline area thins towards the NW and SE at the trough margin of the basin. The Nkporo Group is overlain conformably by the Coal Measure Group consisting of the Mamu, Ajali and Nsukka Formations that form the terminal units of the Cretaceous series. The Benue trough is a linear NE-SW trending intra-continental basin. Structurally, it consists of a series of N-E trending transform fault system, anticlines and synclines. In the Afikpo basin, transform faulting was reactivated during late Maastrichtian terminal tectonic event. The basin was modified by sinisterly strike-slip activity.

The Nkporo Formation in the Afikpo syncline area thins towards the NW and SE at the trough margins of the basin. The Nkporo Formation is the basal formation of the Campanian-Maastrichtian sediments, and is relatively undisturbed but intruded by igneous rocks. High geothermal gradients prevail in this area close to the intrusive. Simple syn-sedimentary growth faults and tectonic structures such as folds and strike-slip faults are present in the Afikpo sub-basin (Odigi, 2007).

The Nsukka Formation consists of deposit of proto-Niger delta, which advanced rapidly southward in the Anambra basin and the Afikpo syncline. The formation ranges from Maestrichtian to probably lower Palaeocene and was deposited during a transgressive phase. Hence, the Nsukka Formation is underlain by the Ajali Sandstone. The Campano- Maastrichtian in south

eastern Nigeria begins with dark gray, often friable, shale with occasional thin beds of limestone and sandstone. This part of the sequence belongs to the Nkporo Formation, the Owelli Sandstone, Enugu shale and Asata shale are lateral equivalents of the Nkporo Formation. These inner basin sediments are all of shallow water origin and there are frequent sharp facie changes. The broad, shallow sea gradually swallowed further and coal-accumulating conditions resulted.

The basal part of the coal measure sequence, previously known as the "Lower Coal Measures" but now known as the Mamu Formation contains marine intercalations composed of ammoniferous shale (Rayment, 1964). The coal being part of the sequence consists of predominantly fresh water and low salinity sandstones, shale, mudstones and sandy shale, coal seams occur at several levels.

Principles of remote sensing

Electromagnetic radiation is a form of energy with the properties of a wave, and its major source is the sun. Solar energy traveling in the form of waves at the speed of light (denoted as c and equals to 3×10^8 m/s) is known as the electromagnetic spectrum. The waves propagate through time and space in a manner rather like water waves, but they also oscillate in all directions perpendicular to their direction of travel. The electromagnetic radiation reaching the earth's surface is partitioned into three types by interacting with features on the earth's surface. Transmission refers to the movement of energy through a surface. The amount of transmitted energy depends on the wavelength and is measured as the ratio of transmitted radiation (I) to the incident radiation (I_0), known as transmittance (T) as in equation (1).

$$T = I \div I_0 \dots\dots\dots (1)$$

Remote sensing systems can detect and record both reflected and emitted energy from the earth's surface. Reflectance (R) is the term used to define the ratio of the amount of electromagnetic radiation (Er) reflected from a surface to the amount originally striking the surface (Eo) as in equation (2).

$$R = Er \div Eo \dots\dots\dots (2)$$

When a surface is smooth, we get specular reflection, where all (or almost all) of the energy is directed away from the surface in a single direction. When the surface is rough and the energy is reflected almost uniformly in all directions, diffuse reflection occurs. Most features of the earth's surface lie somewhere between perfectly specular or perfectly diffuse reflectors. Whether a particular target reflects specularly or diffusely or somewhere in between depends on the surface roughness of the feature in comparison with the wavelength of the incoming radiation. If the wavelengths are much smaller than the

surface variations or the particle sizes that make up the surface, diffuse reflection will dominate. Some electromagnetic radiation is absorbed through electron or molecular reactions within the medium. A portion of this energy then is re-emitted, as emittance, usually at longer wavelengths, and some of it remains and heats the target. For any given material, the amount of solar radiation that reflects, absorbs, or transmits varies with the wavelength. This important property of matter makes it possible to identify different substances or features and separate them by their spectral signatures (spectral curves).

MATERIALS AND METHODS

Landsat data source

The landsat data used were the NigeriaSat-2 images acquired in April 2012 from the National Space Research and Development Agency (NASRDA). The images were obtained using landsat ETM sensor with band combinations 2, 3 and 4 with a resolution of 30 m. The following color codes were used: red for vegetation, black for rock outcrops, grey/white for bare/exposed surfaces and blue for water bodies.

Data processing

The processing of the LandSat data were done using ILWIS 3.2 Academic and ERDAS imaging software. The software have the capacities of carrying out various data enhancement techniques such as linear enhancement, statistical analysis, principal component analysis and normalized difference vegetation index. The image enhancement operations were carried out for better visual interpretation, to reduce noise distortion in the image prior to a multi-band image classification and to detect line features in the satellite image to aid structural interpretation. The images were Geo-referenced to a Universal Transverse Mercator (UTM) grid using the software to allow compatibility and comparison with other data sets.

RESULT, INTERPRETATION AND DISCUSSION

Normalized Difference Vegetation Index (NDVI) of the area

The Normalized Difference Vegetation Index (NDVI) is an index of plant "greenness" or photosynthetic activity, and is one of the most commonly used vegetation indices. Vegetation indices are based on the observation that different surfaces reflect different types of light differently. Photosynthetically active vegetation, in particular,

absorbs most of the red light that hits it while reflecting much of the near infrared light. Vegetation that is dead or stressed reflects more red lights and less near infrared light. Likewise, non-vegetated surfaces have a much more even reflectance across the light spectrum. By taking the ratio of red and near infra-red bands from a remotely-sensed image, an index of vegetation "greenness" can be defined. The Normalized Difference Vegetation Index (NDVI) is probably the most common of these ratio indices for vegetation. NDVI is calculated on a per-pixel basis as the normalized difference between the red and near infra-red bands from an image.

Mathematically, NDVI calculation on per-pixel basis is given as:

$$NDVI = \frac{NIR-RED}{NIR+RED}$$

where NIR is the near infra-red band value for a cell, RED is the red band value for the cell and thus

NDVI can be calculated for any image that has a red and a near infra-red band.

The biophysical interpretation of NDVI is the fraction of absorbed photosynthetically active radiation. Many factors affect NDVI values like plant photosynthetic activity, total plant cover, biomass, plant and soil moisture, and plant stress. Because of this, NDVI is correlated with many ecosystem attributes that are of interest to researchers and managers (e.g. net primary productivity, canopy cover, bare ground cover). Also, because it is a ratio of two bands, NDVI helps compensate for differences both in illumination within an image due to slope and aspect, and differences between images due to things like time of day or season when the images were acquired. Thus, vegetation indices like NDVI make it possible to compare images over time to look for ecologically significant changes.

Due to the relationship between many ecosystem parameters, NDVI has been of widespread use in solving ecological problems. The uses include assessing or monitoring vegetation dynamics or plant phenological changes over time, biomass production, carbon sequestration or CO₂ flux, changes in rangeland condition and soil moisture vegetation or land cover classification

Values of NDVI in the map normally range from -1.0 to +1.0, but values less than zero typically do not have any ecological meaning, so the range of the index is truncated to 0.0 to +1.0. Higher values signify a larger difference between the red and near infra-red radiation recorded by the sensor - a condition associated with highly photosynthetically-active vegetation. Low NDVI values mean there is little difference between the red and NIR (near infra-red) signals. This happens when there is little photosynthetic activity, or when there is just very little NIR light reflectance (i.e. water reflects very little NIR light).

From the NDVI map of the study area, (Figure 2) the Northern region can be visibly spotted as areas with NDVI of - 0.24 – 0.08, which shows an unhealthy vegetation. The area were much earlier in time protected

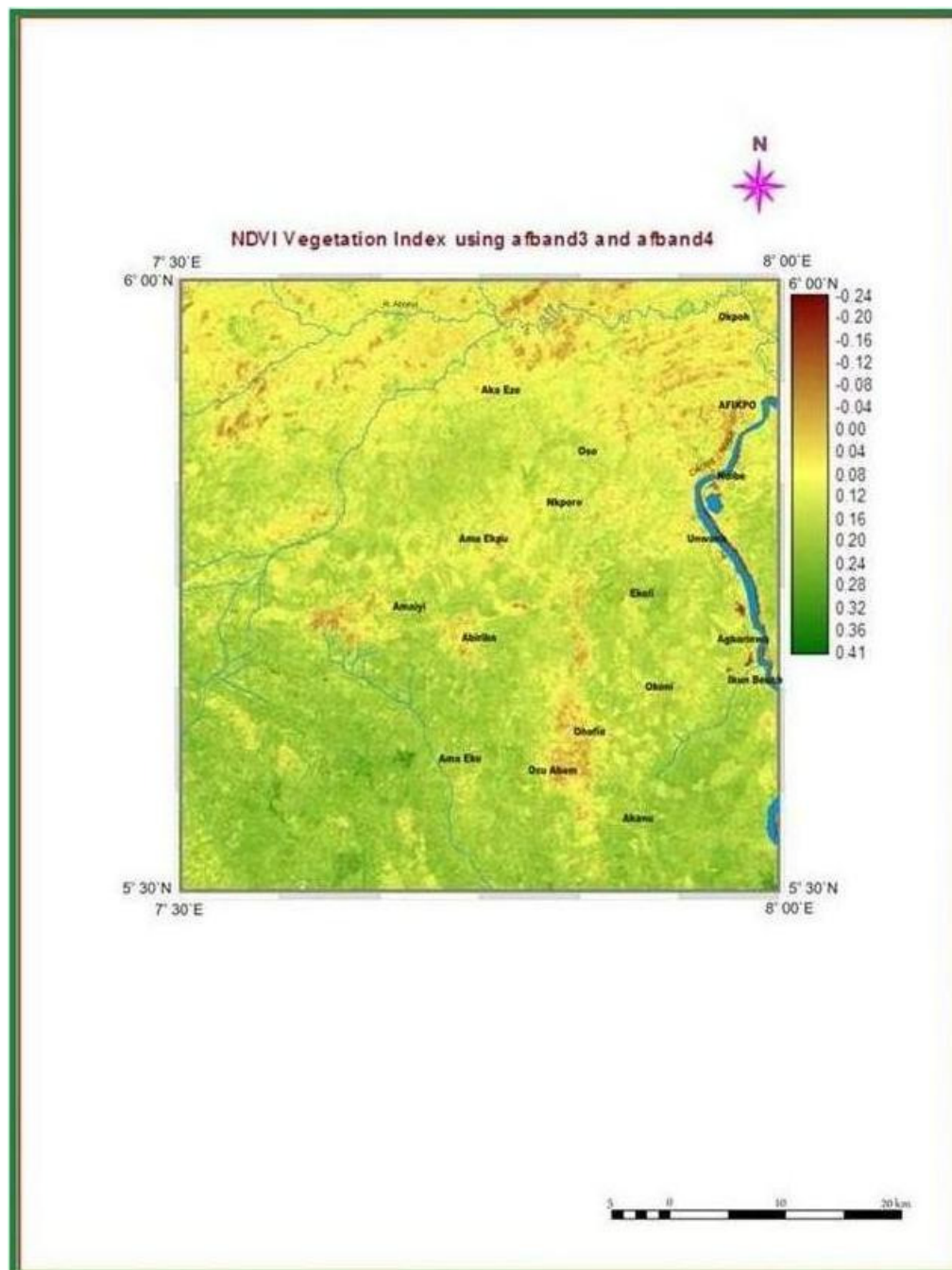


Figure 2. Normalized difference vegetation index (NDVI) Map

by dense forest cover which the inhabitants removed in the process of urbanization and agricultural activities leading to an exposure of the fragile soil to the heavy downpour and concentrated runoff of the area. The high speed of the surface runoff culminates in rapid washing away of the soil surface and weakening the soil strata which can cause gullies in the area. The south-west region was revealed to have the highest vegetation with an NDVI of 0.20-0.41.

Digital Elevation Model (DEM)

Figure 3, shows the topographic roughness and geomorphologic structure of the study area. The DEM is employed for structural geologic and tectonic interpretations such as locating faults, drainage pattern, geomorphology, plate positions slope, lineaments and the boundary between geologic units. The DEM of the study area (Figure 3) shows the elevation differences and a

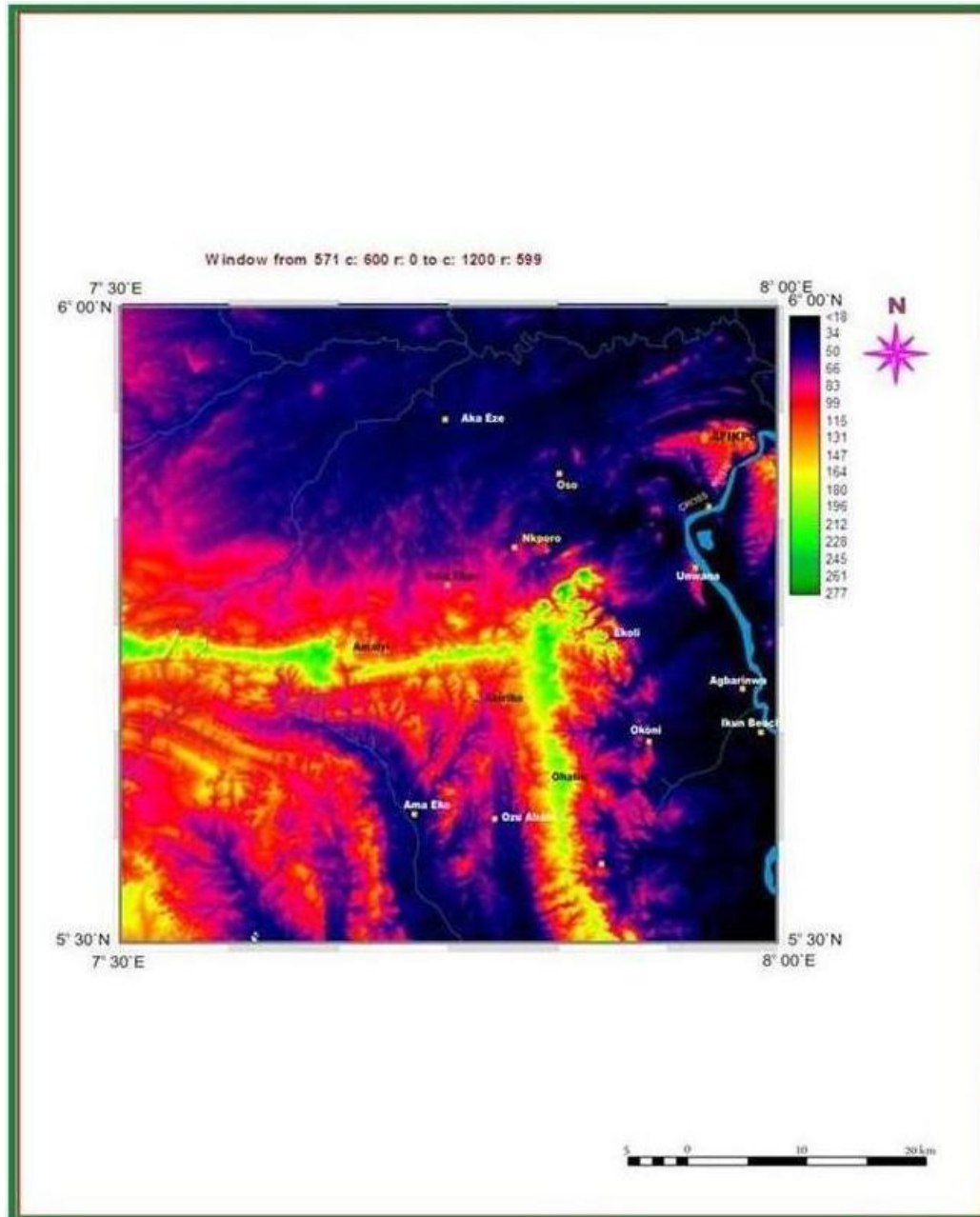


Figure 3. The Digital Elevation Model (DEM) of the area

quick estimation of the morphology of the area. From the DEM map, the area is characterized by a rugged topography. The difference in elevation of the area is very consistent.

From the Figure 3, the elevation in the South-West region was discovered to have high elevations and large coverage with high lands ranging from 162 - 277 meters above sea level. The central area was noticed to have the highest elevation which and peak of 228 - 277 meters with trend in the East-West direction. The Northern part records a low elevation of 34 - 66 meters above sea

level. While the North-East and the South-East region has the lowest elevation records of less than 18 - 50 meters above sea level. The elevation of the area is increasing as you move from the north-eastern part to the south-western part of the area and it is characterized by low hills with steep slopes which when correlated with the intense rainfall can be a causative factor for gully erosion in the area.

The dendritic drainage pattern of the area trends in the NE-SW direction (Figure 3) is associated with trench branching tributaries joining the main stream at acute

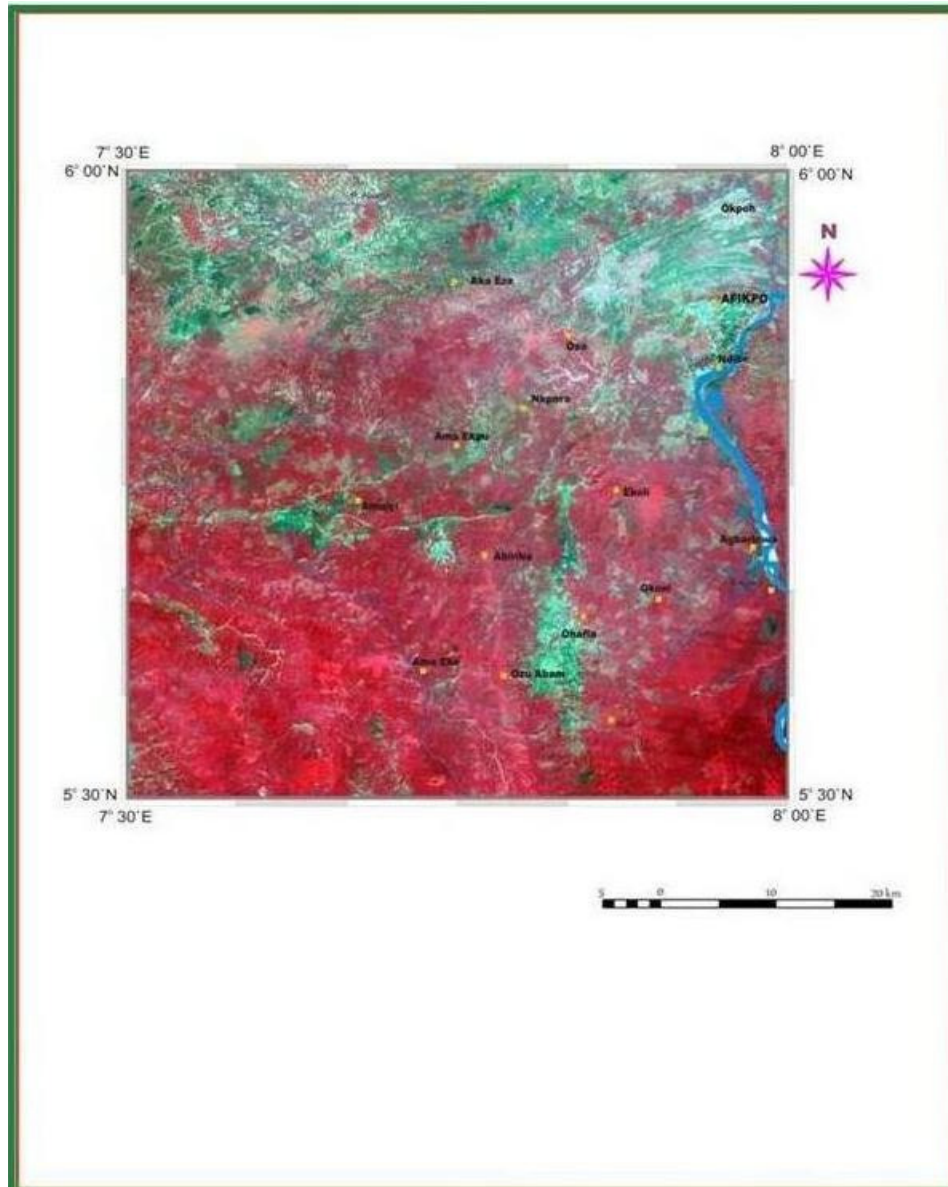


Figure 4. False color composite map of the area

angle and this pattern shows up on homogeneous, uniform soil and rock materials mostly in soft sedimentary rocks and old dissected coastal plains (Howard, 1967). The dendrite pattern reveals a lithological, structural and topographical homogeneity of the study area. This occurs on homogenous gentle, uniformly sloping sedimentary surfaces whose main collector streams may indicate a fault or fracture.

Color composite map analysis

Color and color tone are the brightness levels in digital images. The reflection of color tones of different materials

on the earth helps in distinguishing surface materials and their boundaries. In this study, there are two false color composite images (Figures 4, 5 and 6) with RGB (R = Red, G = Green B = Blue bands of Landsat 2 Thematic Mapper (TM) multi spectral image respectively. The mid infra-red portion of the spectrum is sensitive to active vegetation, water bodies and soil moisture. The composite image provides a naturalistic and earth view of the landscape of the study area.

False color composite map

In Figure 4, the red areas represent active vegetations

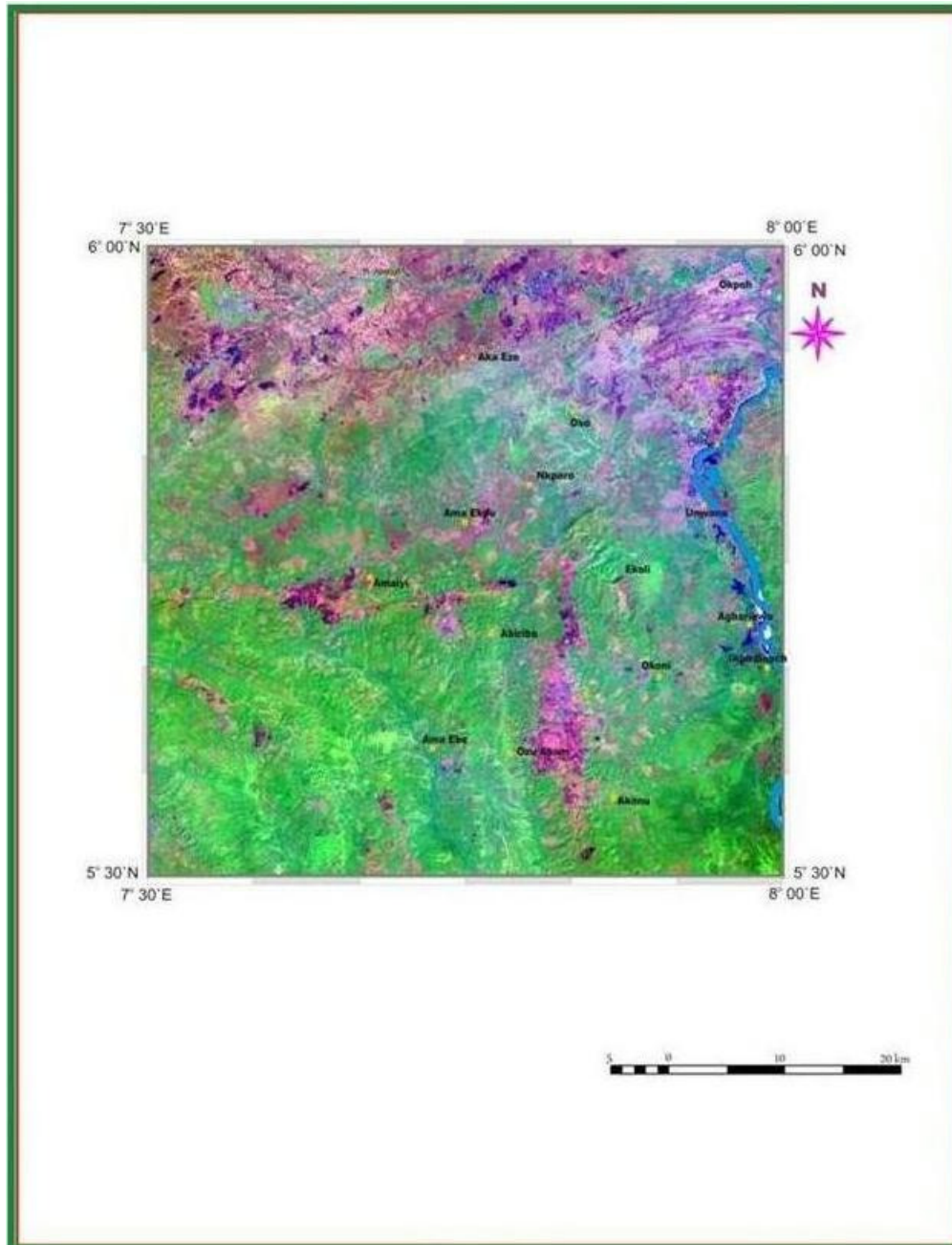


Figure 5. True color composite map of the area.

which include trees and bushes, the grey areas represent the ground surface or bare rocks which are usually the urban areas. While the green areas represents the active vegetation and the blue represents water bodies.

True color composite Map

In Figure 5, it is shown that the olive green color signifies regions of high vegetations, the medium to light green

region indicates farm lands, dark green indicates wetland vegetations, light blue regions show the urban areas and bare soil, while the shades of blue represents the drainage channels.

Geocover map

From Figure 6, shades of green are used to represent regions of high vegetations, farm lands and wetland vegetation. Lavender and pale pink color indicates urban

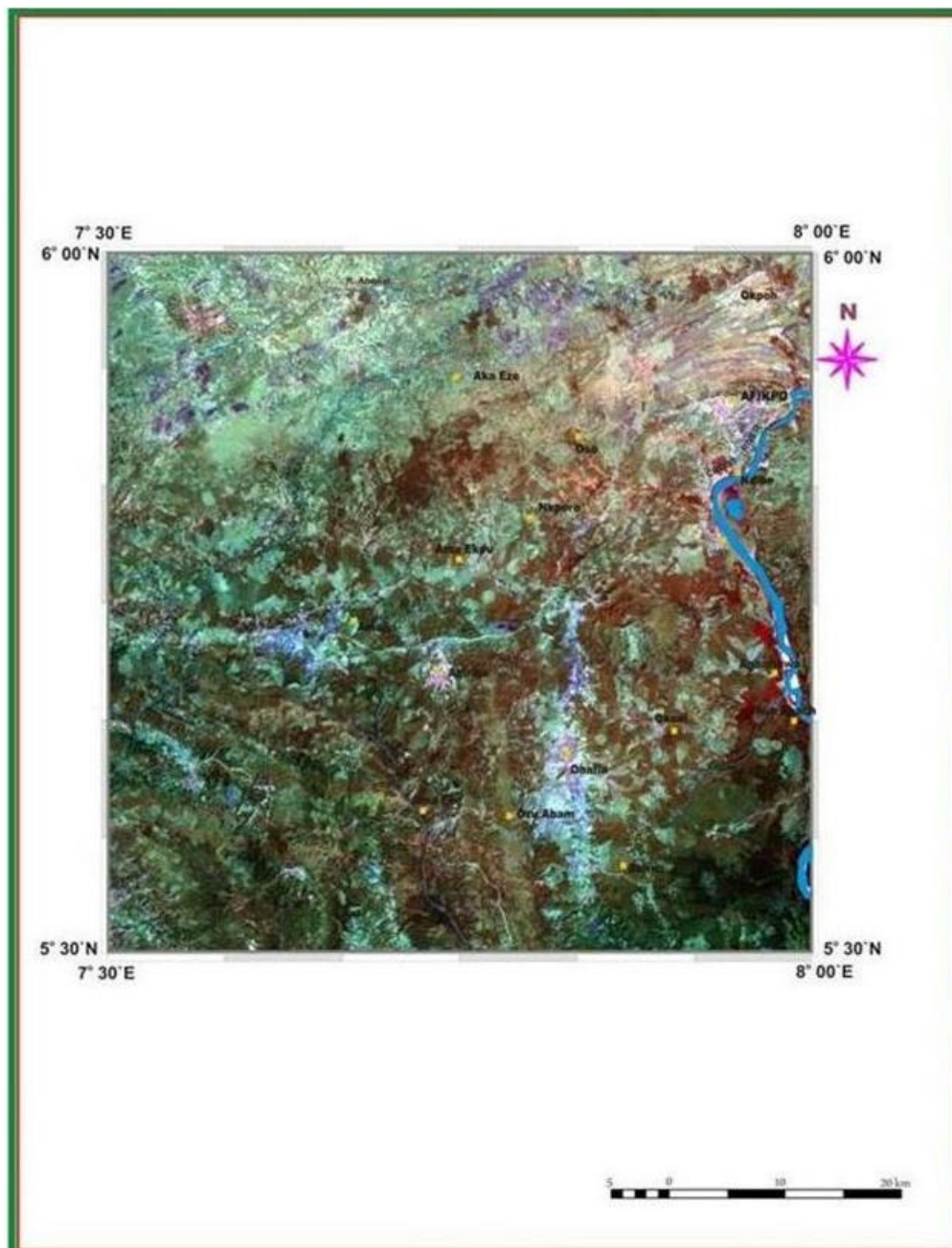


Figure 6. Geo-cover map the study area

areas and bare soil, while black to dark blue indicates water bodies.

Lineament analysis of the study area

Lineaments are linear features in a landscape which is an expression underlying geological structures such as faults. Areas with high lineament density indicates the closeness of the basement (underlying rocks) to the earth surface and becomes a possible mineral deposit, while

areas with lesser lineament density indicates plane grounds mainly composed of sedimentary rocks and therefore becomes a possible site for hydrocarbon reservoir if other ground truths are considered. The geological interpretation of the Landsat imagery revealed a number of lineaments and mega lineaments over 15 km in size trending in the NE–SW, N–S, and NW–SE directions (Figures 7 and 8).

It shows that the north-east region and the central region of the area has the highest lineament concentration therefore its basement is closer to the

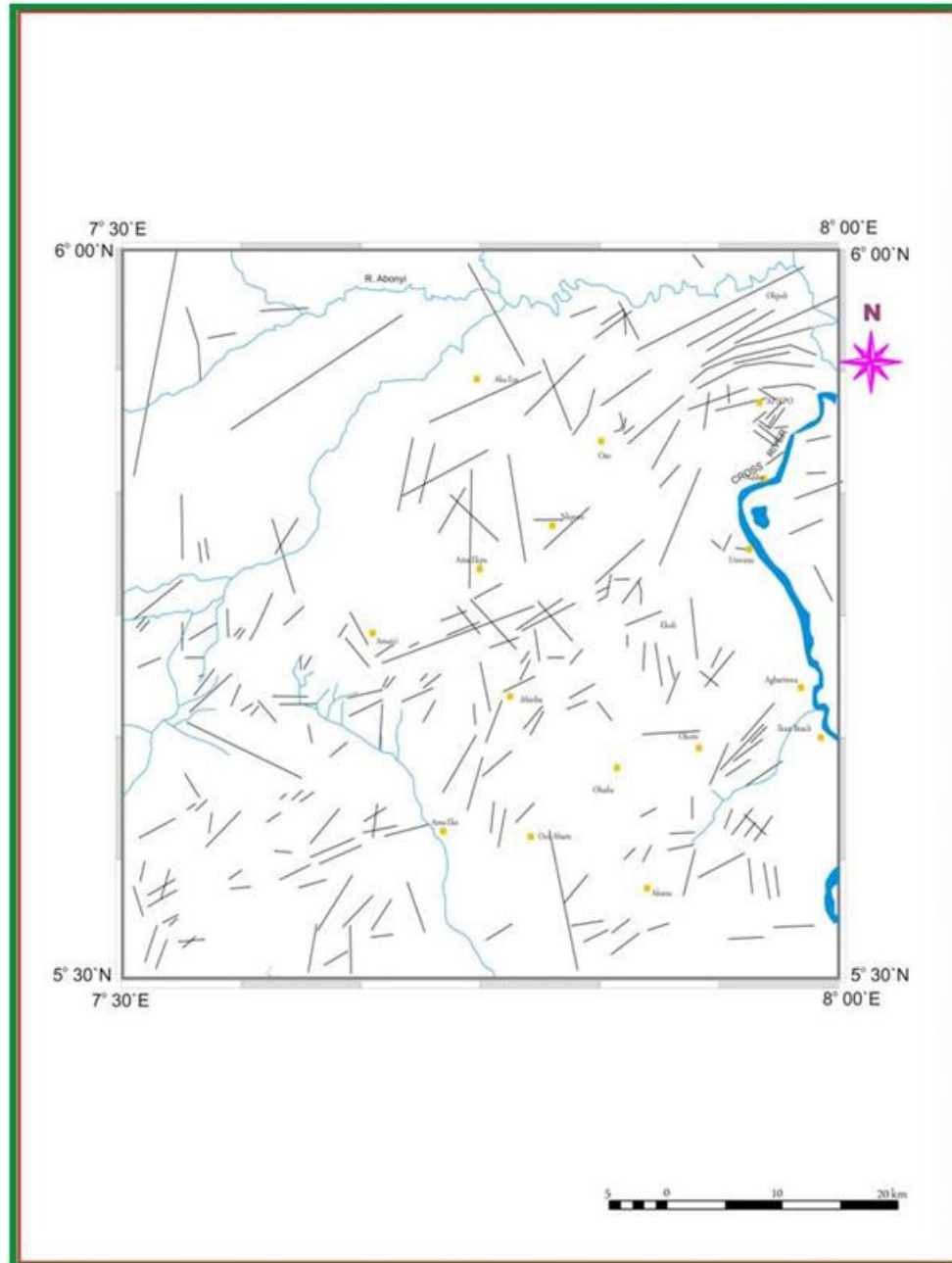


Figure 7. Lineament map of the study area

surface of the earth; this implies that it could be a possible mineral deposit site. Also the north-west region of the region has the lowest lineament concentration which implies that it is composed of plain sedimentary rocks of sand stones and therefore could be a possible hydrocarbon reservoir if other ground truths are in place. The trend surface analysis of the tectonic and structural features of the area in relation to the interpreted lineaments which ranges from the rose diagram revealed surface trend of NE–SW, NW–SE, N–S and E–W directions with the dominant structural trends being in the

NE–SW and the NW–SE which corresponds to the major lineament trend of the Afikpo sub-basin. This shows that the area has a rugged topography and it is partly deformed by tectonic processes.

Rose diagram

The rose diagram or Azimuth frequency diagram is a diagram that shows the direction of the dominant lineament trend in the area of study. The data gotten from

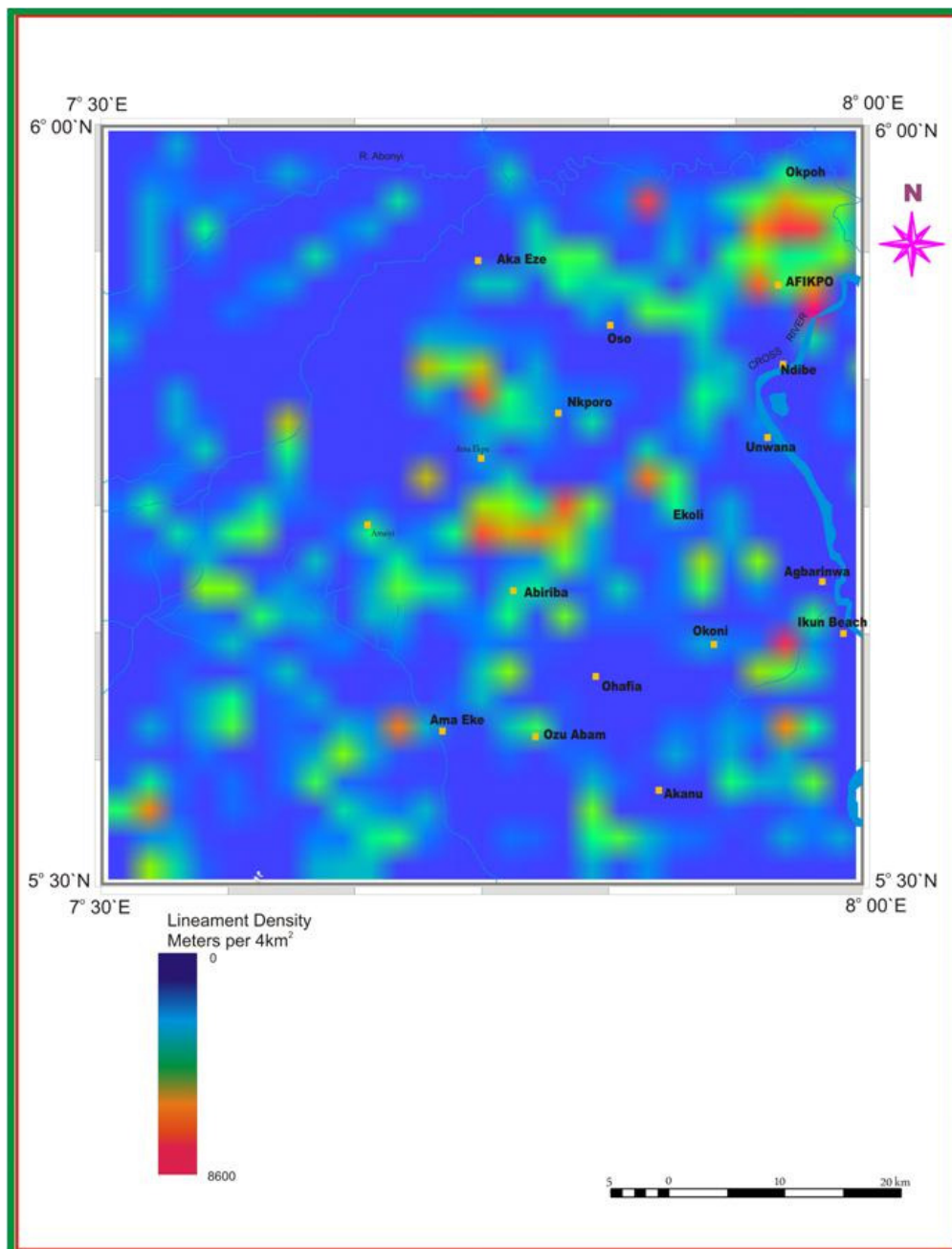


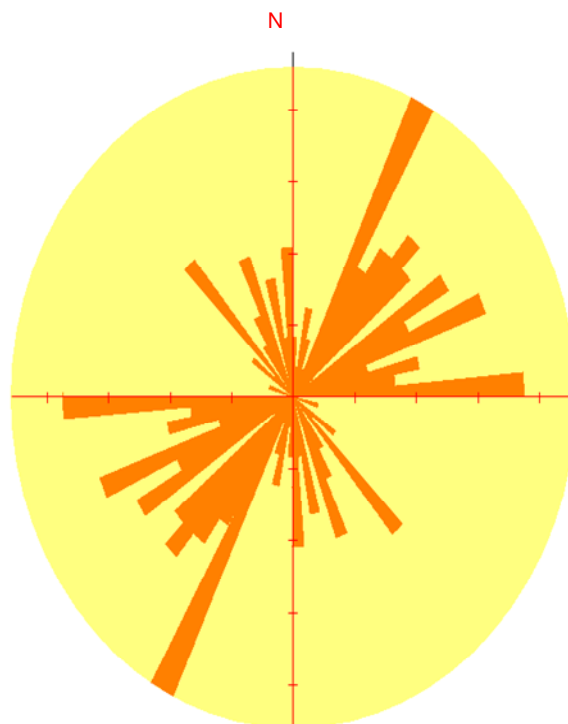
Figure 8. Lineament density of the study area.

Table 1. Landsat data with their spectral and spatial resolutions

154 SE – 334NW	175 SSE – 355 NNW	070 ENE – 250 WSW	090 E – 270 W
020NNE – 200 SSW	050 NE – 230 SW	155 SE – 335 NW	060 NE – 240 SW
015 NNE – 195 SSW	015 NNE – 195 SSW	035 NE – 215 SW	060 NE – 240 SW
055 NE – 235 SW	070 ENE – 250 WSW	065 NE – 245 SW	060 NE – 240 SW
085 ENE – 265 WSW	135 SE – 315 NW	082 ENE – 262 WSW	084 ENE – 264 WSW
040 NE – 220 SW	075 ENE – 255 WSW	080 ENE – 260 WSW	080 ENE – 260 WSW
090 E – 270 W	0 N – 180 S	160 SSE – 340 NNW	150 SE – 330 NW
140 SE – 320 NW	035 NE – 215 SW	050 NE – 230 SW	0 N – 180 S
005 NNE – 185SSW	065 NE – 245 SW	065 NE – 245 SW	035 NE – 215 SW

Table 1 Continues

090 E – 270 W	090 E – 270 W	0 N – 180 S	085 ENE – 265 WSW
170 SSE – 350 NNW	0 N – 180 S	028 NE – 208 SW	030 NE – 210 SW
150 SE – 330 NW	070 ENE – 250 WSW	040 NE – 220 SW	160 SSE – 340 NNW
041 NE – 221 SW	040 NE – 220 SW	075 ENE – 255 WSW	080 ENE – 260 WSW
028 NE – 208 SW	028 NE – 208 SW	050 NE – 230 SW	010 NNE – 190 SSW
012 NNE – 192 SSW	130 SE – 310 NW	140 SE – 320 NW	0 N – 180 S
030 NE – 210 SW	175 SSE – 355 NNW	040 NE – 220 SW	090 E – 270 W
050 NE – 230 SW	028 NE – 208 SW	110 ESE – 290 WNW	060 NE – 240 SW
035 NE – 215 SW	160 SSE – 340 NNW	090 E – 270 W	090 E – 270 W
140 SE – 320 NW	040 NE – 220 SW	030 NE – 210 SW	030 NE – 210 SW
170 SSE – 350 NNW	060 NE – 240 SW	030 NE – 210 SW	030 NE – 210 SW
065 NE – 245 SW	070 ENE – 250 WSW	060 NE – 240 SW	090 E – 270 W
160 SSE – 340 NNW	064 NE – 244 SW	070 ENE – 250 WSW	075 ENE – 255 WSW
080 ENE – 260 WSW	070 ENE – 250 WSW	140 SE – 320 NW	040 NE – 220 SW
140 SE – 320 NW	140 SE – 320 NW	130 SE – 310 NW	070 ENE – 250 WSW
070 ENE – 250 WSW	080 ENE – 260 WSW	160 SSE – 340 NNW	0 N – 180 S
160 SSE – 340 NNW	0 N – 180 S	030 NE – 210 SW	050 NE – 230 SW
030 NE – 210 SW	030 NE – 210 SW	060 NE – 240 SW	0 N – 180 S
035 NE – 215 SW	0 N – 180 S	090 E – 270 W	170 SSE – 350 NNW
170 SSE – 350 NNW	040 NE – 220 SW	040 NE – 220 SW	042 NE – 222 SW
043 NE – 223 SW	040 NE – 220 SW	043 NE – 223 SW	050 NE – 230 SW

**Figure 9.** Rose diagram of the study area showing the dominant lineament trends.

Number of data plotted = 120

Sector Interval Angle = 5°

Scale spacing = 2% [2 data]

Maximum = 9.2% [11 data]

Mean Resultant direction = 043

Circular Mean Dev. = 44°

basin associated with two major fault lines trending NE-SW and NW-SE (Ehirim and Ebeniro, 2006). These findings are also in line with the aeromagnetic results which show that the area is affected by tectonic activities and the effect of these tectonic activities on the geologic formation of the area is responsible for the increasing gully and land sliding in the study area. Results from the lineament analysis revealed that the lineament trends in the area correlated well with the measured strikes of the geologic formations as in Figure 1.

CONCLUSION

The study on Afikpo sub-basin shows that the reservoir quality varies from marginal to intermediate in the west to poor in the east, with predictable trends being directly linked to depositional environment and diagenesis. The Nkporo Formation consists of basically sandstones, shale and coal. The formation is considered to be relatively a good source rock. The Nkporo Formation of the sub-basin has shown that the formation consists of tidal estuarine sandstones and mudstones of unstable shoreline setting overlain by regional marine shale deposits that suggest a stable paleogeographic setting. The dominantly sandy Afikpo Sandstone, comprising mainly sandstones, dark grey shales and coals represents an incised valley fill deposited under tidally influence estuarine setting. The formation comprises estuarine point bars/tidal channels in retrograding bay head; central estuarine shale, carbonaceous facies and fine sandstones and siltstones in bay fill/lagoons and barrier and tidal sand bars in the estuary mouth and littoral foreshore - upper shore face setting and has been rated as a possible hydrocarbon reservoir basin that is worthy of attention. Tectonic features such as folds and strike-slip faults are present in the Ajali Formation which implies that the area is prone to gully erosion.

Mamu Formation was seen to have the highest high lands in the area with the most dense lineaments which implies that the basement in the area is close the surface of the earth. This shows that the formation possesses some minerals such as coal and also is not a favorable site for borehole drilling. The Mamu Formation has the capability to generate and expel liquid hydrocarbons and gases as part of an active Cretaceous petroleum system.

RECOMMENDATIONS

From the various interpretations of the LandSat imagery of the Afikpo sub-basin, it was discovered that the center and the East-West regions of the sub-basin which comprised of towns such as Amayi, Abiriba, Ohafia, Ekoli and Afikpo, are high lands between 147-277 meters above sea level. This implies that the basements are

close the earth surface in the region and in turn are possible sites for mineral explorations.

Also, areas around Cross River, which comprised towns like Agbarinwa and Ikun beach and the northern region comprising of Aka Eze town and areas in the Asu river group have low lands between less than 18-50 meters above sea level. This implies that the basements in the region are far from the earth surface, which in turn infers that the region under investigation can be a possible hydrocarbon deposit.

Based on the above findings, I hereby urge other relevant agencies and the Federal Government to undertake further research such as seismic, resistivity or gravity studies on this area to ascertain this inference, which if found to be true will enhance the economic growth of the country.

REFERENCES

- Ahmad M (1980). Lineaments and their tectonic significance in relation to mineral potential in South India (In) *Advances in space exploration*, Vol. 10 Remote sensing in Mineral Exploration, Carter WD, Rowan LC and Huntington (Ed), J.F Pergamon Press, Paris, pp 101 – 104.
- Cushnie JL (1987). The interactive effect of spatial resolution and degree of internal variability within land-cover types on classification accuracies. *Photogrammetric Engr. and Remote Sensing* 8(1): 15-29.
- Danielska DB, Kibitlewski S, Sadurusi A (1986). Geological analysis of the satellite lineaments of the Vistula Delta plain, Zulaway Wislane, Poland (in) *Remote Sensing for Resources Development and Environmental Management*. Damen MCJ, Smit SG and Verstappen HTH Belkema, Rotterdam (Ed), vol.2 pp 579-584
- Ehirim CN, Ebeniro JO (2006). Tectonic trends delineated from drainage lineament analysis and azimuthal resistivity survey: A case study of southeastern Nigeria gully erosion belt. *Global Journal of Pure and Applied Sciences*, 4(1): 21-28.
- Gastellu-Etchegorry JP (1990). An assessment of SPOT X and Landsat MSS data for digital classification of near-urban land cover, *International Journal of Remote Sensing* 11(2): 225-235.
- Hay SI and Lennon JJ (1999). Deriving meteorological variables across Africa for the study and control of vector-borne diseases: A comparison of remote sensing and spatial interpolation of climate, *Tropical Medicine and International Health* 4, 58–71.
- Herbretreau V, Salem G, Souris M (2007). Thirty years of use and improvement of remote sensing applied to epidemiology: From early promises to lasting frustration. *Health and Place*, 13, 400-403.
- Jensen JR (2005). *Digital image processing: a Remote Sensing Perspective*, 3rd ed., Prentice Hall
- Jensen JR (2007). *Remote sensing of the environment: An Earth resource perspective*, 2nd ed. Prentice Hall
- Kogbe CA (1989). *Geology of Nigeria* (Ed). Rock View (Nigeria) limited Zaramaganda, Jos, Nigeria
- Krishnamurty M, Srivastava VC (1980). Tectonic and lineament patterns of the Vindhyan basin based on Landsat imagery data, in *Advances in Space Exploration Vol.10. Remote Sensing and Mineral Exploration*, Carter WD Rowan, LC, Huntington (Ed), JF Pergamon press Paris pp 95-99
- Lian M, Warner RD, Alexander JL, Dixon KR (2007). Using geographic information systems and spatial and space-time scan statistics for a population based risk analysis of the 2002 equine West Nile epidemic in six contiguous regions of Texas. *International Journal of Health Geographics* 6, 42; available at www.ij-healthgeographics.com/content/6/1/42.
- Odigi MI (2011). Diagenesis and reservoir quality of cretaceous sandstones of Nkporo Formation (Campanian) southeastern Benue

- trough, Nigeria. *Journal of Geology and Mining Research* 3(10): 265-280
- Ojo AG and Adesina FA (2007). An assessment of the efficiency of landsat, NigeriaSat-1 and spot images for landuse/landcover analyses in Ekiti west area of Nigeria. *The International Archives of the Photogrammetry, Remote Sensing and Spatial Information Sciences*, Vol. 38, Part II
- Pal M, Mather PM (2003). An assessment of the effectiveness of decision, tree methods for land cover classification. *Remote Sensing of Environment* 86, 554–565.
- Paola JD, Schowengerdt RA (1995). A review and analysis of back propagation neural networks for classification of remotely sensed multispectral imagery. *International Journal of Remote Sensing* 16, 3033–3058.
- Paola JD, Schowengerdt RA (1997). The effect of neural-network structure on a multispectral land-use/land-cover classification. *Photogrammetric Engineering and Remote Sensing* 63, 535–544.
- Reyment RA (1965). *Aspects of the Geology of Nigeria*. University Press: Ibadan, Nigeria.
- Reyment RA and Barber WM (1956). *Nigeria and Camerouns In Lexique Stratigraphique International: Afrique*. 4: 35-39.
- Ruiz MO, Tedesco C and McTighe TJ (2004). Environmental and social determinants of human risk during a West Nile virus outbreak in the greater Chicago area, 2002. *International Journal of Health Geographics* 3, 8–18.
- Ruiz MO, Walker ED, Foster ES, Haramis LD, Kitron UD (2007). Association of West Nile virus illness and urban landscapes in Chicago and Detroit, *International Journ. of Health Geographics* 6, 10–20.
- Sannier CAD, Taylor JC, Campbell K (1998). Compatibility of FAOARTEMIS and NASA Pathfinder AVHRR Land NDVI data archives for the African continent. *International Journal of Remote Sensing* 19, 3441–3450.
- Simpson A (1955). *The Nigerian Coalfield: The Geology of parts of Owerri and Benue Provinces*. *Bull. Geol. Surv. Nig.* 24: 85.
- Townshend JRG, Goff TE, Tucker CJ (1984). Multi-temporal dimensionality of images of the normalized difference vegetation index at continental scales. Submitted to *Trans. IEEE, Geosciences and Remote Sensing*.
- Townshend JRG, Tucker CJ (1984). Objective assessment of advanced very high resolution radiometer data for land cover mapping, *International Journal on Remote Sensing* 5(2): 987-109.
- Wang Y, Zhang X, Liu H, Ruthie HK (1999). Landscape characterization of metropolitan Chicago region by Landsat TM. In *Proceeding of the ASPRS Annual Conference, Portland, Oregon, May 19–21*, pp. 238–247.
- Weng Q (2001). A remote sensing–GIS evaluation of urban expansion and its impact on surface temperature in the Zhujiang Delta, China. *International Journal of Remote Sensing* 22, 1999–2014.
- Weng Q, Lu D, Schubring J (2004). Estimation of land surface temperature/vegetation abundance relationship for urban heat island studies, *Remote Sensing of Environment* 89, 467–483.
- Whiteman A (1982). *Nigeria: Its Petroleum Geology, Resources and Potentials*. Vols. 1 and 2. Graham and Trotman Ltd.: London. UK.